

# Optical rectification at metal surfaces

Filip Kadlec and Petr Kužel

*Institute of Physics, Academy of Sciences of the Czech Republic, Na Slovance 2, 182 21 Prague 8, Czech Republic*

Jean-Louis Coutaz

*Laboratoire d'Hyperfréquences et de Caractérisation, Université de Savoie, 73376 Le Bourget du Lac Cedex, France*

Received July 13, 2004

The emission of freely propagating terahertz (THz) radiation coming from optical rectification at metallic surfaces has been detected and characterized for the first time to the authors' knowledge. The observed THz transients are induced through nonlinear electronic processes at gold and silver surfaces on intense pulsed optical photoexcitation and exhibit a peak electric field of as much as 200 V/cm. This finding opens a qualitatively new way to investigate nonlinear phenomena at metal surfaces and also can be exploited for the development of new THz emitters. © 2004 Optical Society of America

OCIS codes: 320.7130, 240.4350.

The terahertz (THz) spectral range has been an active field of research for the past two decades. This research has been stimulated by the development of ultrafast lasers and of the gated emission and detection techniques that facilitated the introduction of so-called time-domain THz spectroscopy. This technique, in addition to well-established spectroscopic investigations (see, e.g., Refs. 1 and 2 for reviews), has been successfully used in THz imaging, tomography, and sensing applications.<sup>3,4</sup> All this progress has been made possible by the development and optimization of efficient active devices such as THz emitters and sensors. The most widely used methods for pulsed THz emission involve photoconductive switching in biased semiconductor antennas and optical rectification (OR) in nonlinear crystals. THz generation by OR in nonlinear dielectrics was demonstrated 20 years ago by Auston *et al.*<sup>5</sup> A recent review of broadband and narrowband THz emitters can be found in Ref. 3. Other techniques, such as magnetic-field enhancement of the THz generation in semiconductor surface depletion fields<sup>6</sup> and emission from metal–semiconductor Schottky barriers,<sup>7</sup> from superconducting thin films,<sup>8</sup> and recently also from ferromagnetic films,<sup>9</sup> have been discovered and studied. Nevertheless, the lack of high-power and low-cost THz sources still remains a significant limitation of current THz systems.

It is known that at the surface of a metal the electronic density of states exhibits a discontinuity that can give rise to strong anharmonic and nonlinear effects. In the 1960s, second-harmonic generation (SHG) at the surfaces of metals was observed<sup>10</sup> that later was explained through a classic theory of interaction of the incident electromagnetic field with the free electrons in the metal within a nonlocal response framework.<sup>11–14</sup> It was shown<sup>15</sup> that the nonlinear optical response at a metal surface is a sensitive probe of the electronic structure; nevertheless, OR at metal surfaces has not been reported.

In this Letter we attempt to fill this gap partially by presenting, for the first time to our knowledge, experimental data on THz generation at the surfaces of

gold and silver. In principle, OR data can bring information about the second-order nonlinear susceptibility tensor that is complementary to that obtained by SHG, as OR and SHG probe different spectral ranges. At the same time the information is richer because of the phase sensitivity of time-domain spectroscopy: The time dependence of the radiated THz field can be analyzed to reveal the dynamics of underlying nonlinear processes, as in the case of the THz emission spectroscopy that is widely applied in semiconductors<sup>16,17</sup> for investigation of the ultrafast carrier dynamics.

Figure 1 shows the experimental setup. As the laser source we used a Ti:sapphire multipass amplifier (Odin, Quantronix) working at a repetition rate of 1 kHz, providing 1-mJ pulses with a mean wavelength of  $\lambda_0 = 810$  nm, a bandwidth of  $\Delta\lambda = 30$  nm, and duration of  $\Delta t = 50$  fs. Most of the beam power was used for sample excitation, either directly or after SHG in a  $\text{LiB}_3\text{O}_5$  crystal, which raised  $\Delta t$  to  $\sim 100$  fs. A  $\lambda/2$  plate and neutral-density filters were used to control the beam intensity and polarization. Only dielectric-coating mirrors were used up to this point. After  $45^\circ$  reflection on the sample (spot size,  $\approx 4$  mm), the excitation beam was absorbed by a Teflon–polyethylene filter that was transparent to THz radiation. The THz pulses were detected by the usual electro-optic sampling scheme with a 1-mm-thick [011] ZnTe crystal.

In a first series of experiments in ambient air we measured the THz signal as a function of incident

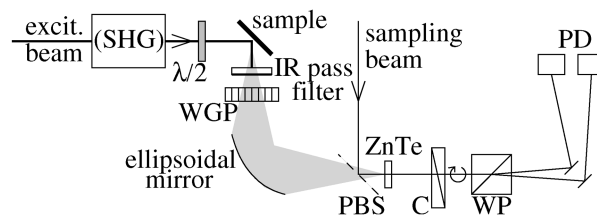


Fig. 1. Schematic of the experimental setup: WGP, wire-grid polarizer; PBS, pellicle beam splitter; C, compensator; WP, Wollaston prism; PD, balanced Si photodiodes.

fluence  $\Phi_0$ . Two samples were used: 99.9% purity bulk silver (Sigma-Aldrich), the surface of which had been polished to reduce chemical contamination of the surface, and a 100-nm-thick Au film deposited by plasma sputtering onto a glass substrate. The temporal waveforms were squared and integrated over time; thus we obtained the values of THz fluence  $\Phi_{\text{THz}}$  shown in Fig. 2. The wire-grid polarizer and the ZnTe crystal were oriented to detect  $p$ -polarized radiation only. We verified that there was no detectable THz signal in the  $s$  polarization— $\Phi_{\text{THz}}$  was at least 3 orders of magnitude below that detected in the  $p$  polarization—for any polarization of the excitation beam ( $p$ ,  $s$ , or intermediate). As in the case of SHG, the nonlinearity is connected to three components of the second-order nonlinear susceptibility,  $\chi_{xxx}$ ,  $\chi_{zxx}$ , and  $\chi_{zzz}$ .<sup>15</sup> As  $\chi_{xxx}$  would give rise to an  $s$ -polarized signal, which we did not observe, we can conclude that there was no substantial in-plane current, because  $\chi_{zzz}$  and  $\chi_{zxx}$  can give rise only to a current normal to the surface.

The most intense THz signal recorded came from Au excited by a  $p$ -polarized 810-nm beam with  $\Phi_0 = 6 \text{ mJ/cm}^2$ . We determined the corresponding value of the peak electric field as  $E = 200 \text{ V/cm}$ . To this purpose, we used another ZnTe crystal as a stronger THz emitter and calibrated the scale of the detection system with respect to the compensator shift. With decreasing  $\Phi_0$ , the THz fluence first remained proportional to  $\Phi_0^2$ ; below  $\Phi_0 = 2 \text{ mJ/cm}^2$  it dropped approximately an order of magnitude below the parabola. With an  $s$ -polarized excitation beam the THz signal was  $\sim 3$  times weaker and the  $\Phi_0$  dependence was similar.

OR on Ag displayed a different behavior. At the highest  $\Phi_0$  used, the THz signal was  $\sim 15$  times weaker than for Au. With decreasing  $\Phi_0$ , it fell much faster than expected:  $\Phi_{\text{THz}}$  is proportional to  $\Phi_0^5$ . The ratio between the signals obtained in  $p$  and  $s$  polarization was  $\sim 2.5$ .

Furthermore, using SHG, we excited the samples at  $\lambda_0 = 405 \text{ nm}$ . In Ag this led to a THz fluence  $\sim 2$  orders of magnitude stronger than for  $\lambda_0 = 810 \text{ nm}$  with a similar excitation fluence, so the signal could be detected for  $\Phi_0$  ranging from a few tenths to  $1 \text{ mJ/cm}^2$  (limited by the SHG efficiency). By contrast, the THz signal generated in Au was weaker than with  $\lambda_0 = 810 \text{ nm}$  by more than 2 orders of magnitude, so all the SHG power was needed to provide a weak measurable signal. In this case,  $\Phi_{\text{THz}}$  appeared somewhat higher with the  $s$ -polarized than with the  $p$ -polarized excitation pulses.

The difference between OR signals for the two metals and excitation wavelengths appears to be surprisingly great. For Ag at both wavelengths and for Au at  $\lambda_0 = 810 \text{ nm}$ , only  $s$  electrons should be at the origin of the nonlinear signal, and the excitation occurs in a region of high reflection (weak absorption). As the values of the dielectric functions in this region do not display substantial differences, one would expect *a priori* similar conversion efficiencies. It is known, however, that various sulfur-containing molecules will form relatively quickly by adsorption

on a Ag surface; this may explain at least partially the differences in  $\Phi_{\text{THz}}(\Phi_0)$  dependence. The low OR signal from Au at  $\lambda_0 = 405 \text{ nm}$  might be linked to the enhanced absorption in this spectral range. Let us note that the conversion efficiency of OR,  $\Phi_{\text{THz}}/\Phi_0^2$ , is close to that of SHG in Au (Ref. 11, Table II) and approximately 1–2 orders of magnitude lower in Ag at  $\Phi_0 \approx 6 \text{ mJ/cm}^2$ .

In a second series of experiments, the geometry was slightly modified: The THz beam propagated from the sample directly to the ZnTe crystal without the ellipsoidal mirror. At the same time, the THz beam was enclosed in a low-pressure ( $10^4$ -Pa) box to prevent absorption of water vapor. Although the signal-to-noise ratio was lower than in the previous setup, this configuration enabled us to measure the far-field THz waveforms  $E(t)$  and to deduce the related surface current  $j(t)$  by means of the expression

$$E(t) \propto \frac{\partial j}{\partial t} * \psi_2(t), \quad (1)$$

where the asterisk denotes convolution and  $\psi_2(t)$  is the response function of the ZnTe crystal, which can be calculated when the THz spectrum of the complex refractive index of ZnTe is known [see Eq. (38) of Ref. 18].

The data for both metals and incident polarizations obtained in the second set of experiments at high optical fluence ( $\Phi_0 = 5.8 \text{ mJ/cm}^2$ ) and  $\lambda_0 = 810 \text{ nm}$  are shown in Fig. 3. One can see that the ratios between maximum values of the individual curves correspond to those between values of appropriate  $\Phi_{\text{THz}}$  obtained in the first series of measurements. The shapes of the curves are similar, except for a scaling factor.

Curves that describe the surface current obtained from the temporal waveforms by use of relation (1) are shown in the inset of Fig. 3. Three contributions to the current can be distinguished: (i) The most important variations of  $j(t)$ , owing to the immediate response of the free electrons to the incident electromagnetic field, occur in the time interval  $-0.4 \text{ ps} \leq t \leq 0.4 \text{ ps}$ . The peak amplitude is apparently reduced with respect to the true current

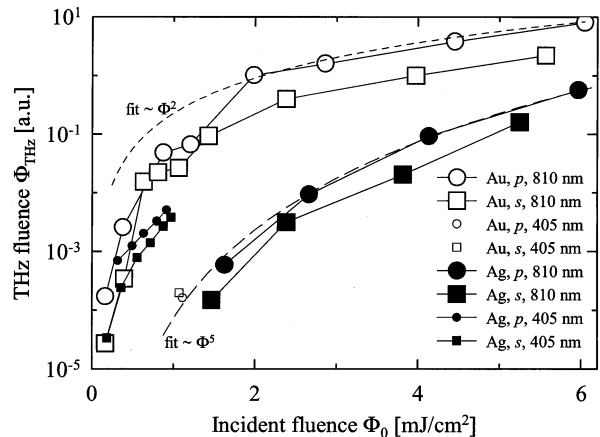


Fig. 2. Integrated THz pulse fluence  $\Phi_{\text{THz}}$  as a function of incident fluence  $\Phi_0$ .  $s$  or  $p$  polarization refers to the excitation beam; experimental errors are less than  $\pm 10\%$  in both coordinates.

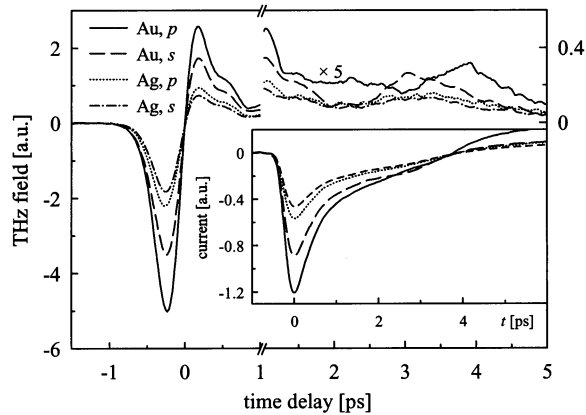


Fig. 3. Far-field THz waveforms measured with 810-nm excitation and  $\Phi_0 = 5.8 \text{ mJ/cm}^2$ . Inset, the corresponding surface current.

because of the limited detection bandwidth of ZnTe; frequencies above 2.5 THz are not detected. The missing high-frequency current explains the positive value of  $j$  at  $t > 4 \text{ ps}$ . (ii) Within  $0.5 \text{ ps} \leq t \leq 3 \text{ ps}$  the variation in current is significantly slower and can be described by an exponential decay with a time constant of  $\sim 4 \text{ ps}$ . (iii) Another clearly detectable change of regime can be observed near  $t \approx 4 \text{ ps}$  for Au and  $p$  polarization and near  $t \approx 3 \text{ ps}$  in the three other cases. These contributions are linked to the small peaks in the  $E(t)$  curves. This effect cannot be due to a parasite reflection of the THz pulse from an optical element in our setup. For confirmation, we performed an independent experiment with a larger-aperture pellicle beam splitter and an IR-pass filter—the only elements between the sample and detector—which had no influence on the presence, shape, or position of the peaks. We tentatively explain the latter two contributions as being due to competition between the retarded THz conductivity and carrier screening effects.

The experimental data presented here reveal the possibility of access to a wealth of new information about the nonlinear properties and electronic structure of metal surfaces. Whereas the physical origin of OR is analogous to that of SHG, calculating the nonlinear optical response of a metal surface from first principles remains difficult. Since the initial studies by Bloembergen *et al.*,<sup>11</sup> the hydrodynamic formalism has been developed for more than three decades and, consequently, the experimental data about OR might be useful for verifying its validity. Because in the present research control over the chemical state of the surface was limited, an improvement of the experi-

mental conditions appears to be a prerequisite for comparison of theoretical and experimental results.

This research was supported by the Czech Academy of Sciences (project AVOZ01-010-914) and by the Ministry of Education of the Czech Republic (project LN00A032). F. Kadlec's e-mail address is kadlecf@fzu.cz.

*Note added in proof:* A work demonstrating THz emission from Fe thin films has appeared since the acceptance of our Letter.<sup>19</sup>

## References

1. G. Grüner, ed., *Millimeter and Submillimeter Wave Spectroscopy of Solids* (Springer-Verlag, Berlin, 1998).
2. C. A. Schmuttenmaer, *Chem. Rev.* **104**, 1759 (2004).
3. B. Ferguson and X.-C. Zhang, *Nature Mater.* **1**, 26 (2002).
4. D. Mittleman, *Sensing with Terahertz Radiation* (Springer-Verlag, Berlin, 2003).
5. D. H. Auston, K. P. Cheung, J. A. Valdmanis, and D. A. Kleinman, *Phys. Rev. Lett.* **53**, 1555 (1984).
6. H. Ohtake, H. Murakami, T. Yano, S. Ono, N. Sarukura, H. Takahashi, Y. Suzuki, G. Nishijima, and K. Watanabe, *Appl. Phys. Lett.* **82**, 1164 (2003).
7. Y. Jin, F. Ma, G. A. Wagoner, M. Alexander, and X.-C. Zhang, *Appl. Phys. Lett.* **65**, 682 (1994).
8. J. L. W. Siders, S. A. Trugman, F. H. Garzon, R. J. Houlton, and A. J. Taylor, *Phys. Rev. B* **61**, 13,633 (2000).
9. E. Beaurepaire, G. M. Turner, S. M. Harrel, M. C. Beard, J.-Y. Bigot, and C. A. Schmuttenmaer, *Appl. Phys. Lett.* **84**, 3465 (2004).
10. F. Brown, R. E. Parks, and A. M. Sleeper, *Phys. Rev. Lett.* **14**, 1029 (1965).
11. N. Bloembergen, R. K. Chang, S. S. Jha, and C. H. Lee, *Phys. Rev.* **174**, 813 (1968).
12. H. R. Jensen, R. Reinisch, and J. L. Coutaz, *Appl. Phys. B* **64**, 57 (1997).
13. J. A. Maytorena, W. L. Mochán, and B. S. Mendoza, *Phys. Rev. B* **57**, 2580 (1998).
14. J. A. Maytorena, B. S. Mendoza, and W. L. Mochán, *Phys. Rev. B* **57**, 2569 (1998).
15. W. Hübner, K. H. Bennemann, and K. Böhmer, *Phys. Rev. B* **50**, 17,597 (1994).
16. P. U. Jepsen, R. H. Jacobsen, and S. R. Keiding, *J. Opt. Soc. Am. B* **13**, 2424 (1996).
17. H. Němec, A. Pashkin, P. Kužel, M. Khazan, S. Schnüll, and I. Wilke, *J. Appl. Phys.* **90**, 1303 (2001).
18. H. Němec, F. Kadlec, and P. Kužel, *J. Chem. Phys.* **117**, 8454 (2002).
19. D. J. Hilton, R. D. Averitt, C. A. Meserole, G. L. Fisher, D. J. Funk, J. D. Thompson, and A. J. Taylor, *Opt. Lett.* **29**, 1805 (2004).